Journal of Catalysis **206,** 60–70 (2002)
doi:10.1006/jcat.2001.3470, available online at http://www.idealibrary.com on IDEAL®

Alumina-Supported Cu–Ag Catalysts for Ammonia Oxidation to Nitrogen at Low Temperature

Lu Gang,*,[1] B. G. Anderson,* J. van Grondelle,* R. A. van Santen,* W. J. H. van Gennip,* J. W. Niemantsverdriet,* P. J. Kooyman,† A. Knoester,‡ and H. H. Brongersma‡

*Schuit Institute of Catalysis, Laboratory of Inorganic Chemistry and Catalysis, Eindhoven University of Technology, P.O. Box 513, 5600 MB, Eindhoven, The Netherlands; †National Centre for High Resolution Electron Microscopy, Delft University of Technology, Rotterdamsweg 137, 2628 AL Delft, The Netherlands; and ‡Calipso B. V., Eindhoven University of Technology, P.O. Box 513, 5600 MB, Eindhoven, The Netherlands

Received June 11, 2001; revised November 2, 2001; accepted November 13, 2001

The addition of copper to alumina-supported silver catalysts, by co-incipient wetness impregnation, increased the selectivity to nitrogen during the catalytic oxidation of ammonia at 250°C without significant decrease in activity relative to that of Ag/alumina alone. An increase in selectivity from 80 to circa 95% was observed at 100% ammonia conversion at the optimum Ag/Cu weight ratio (between 1 : 1 and 3 : 1). No increase in activity was observed for mechanical mixtures of Cu/alumina and Ag/alumina catalysts. Based on transmission electron microscopy (TEM), energy-dispersive X-ray spectroscopy (EDX), low-energy ion-scattering spectroscopy, X-ray photoelectron spectroscopy, and Auger analysis, the catalysts consisted of monolayers of copper oxide on alumina upon which silver particles sat. TEM images and EDX analysis showed that silver particles, with a very large size distribution, existed on all catalysts. EDX also revealed the presence of very small (<1 nm) silver dispersed in copper everywhere on the alumina surface. Thus intimate contact between copper and silver on alumina-supported Cu–Ag catalysts existed. No indication of the formation of $CuAl_2O_4$ or of Cu–Ag phases was observed. The promotional effect of copper can be explained by a bifunctional mechanism in which the silver component mainly catalyzes ammonia oxidation to NO, the first step of this reaction, and the copper catalyzes the selective catalytic reduction of NO to nitrogen, thus reducing N_2O formation on silver.

Key Words: **ammonia; oxidation; silver; copper; supported catalyst.**

1. INTRODUCTION

The increasing problem of air pollution by N-containing compounds, such as NO, NO_2, N_2O, and NH_3, has led to more stringent emissions control. The removal of ammonia from waste streams is becoming an increasingly important issue. Selective catalytic oxidation (SCO) of ammonia to nitrogen and water could be a solution to pollution caused by various ammonia emission sources, such as the selective catalytic reduction (SCR) process, soda production, and agricultural sources (1–12).

Most studies on ammonia oxidation focus on the high-temperature (>800 K) process that selectively produces NO because of its industrial importance. However the low-temperature reaction that mainly produces N_2 and N_2O is becoming more important because of the environmental aspect. Various catalysts of different types have been tested for the low-temperature ammonia oxidation reaction: biological catalysts (1, 2), metal oxide catalysts (3–6), ion-exchanged zeolites (7–9), and metallic catalysts (10–12). When the various types of catalysts are compared it turns out that the metallic catalysts such as Pt, Ir, and Ag are the most active but the least selective. Significant amounts of N_2O are produced on these catalysts. The metal oxide catalysts such as CuO, V_2O_5, and MoO_3 show very high selectivity to nitrogen, but the reaction temperature needed is too high to be matched with some industrial applications.

We previously reported that silver was very active for ammonia oxidation (13). Alumina-supported silver catalysts were superior even to noble metal catalysts in both activity and selectivity to nitrogen. However the nitrogen selectivity of the silver-based catalysts (circa 80%) is not sufficient, as N_2O and NO are still coproduced. As these compounds are even more toxic than NH_3, selectivity to nitrogen of near 100% is required. Intermediate species and reaction pathways for ammonia oxidation on an unsupported silver powder catalyst were studied by temperature-programmed desorption, temperature-programmed reduction, Fourier transform–Raman, and transient as well as steady-state ammonia oxidation experiments (14). NO was found to be the main reaction intermediate that produced N_2O as well as N_2. NO could even be formed at room temperature. Its subsequent oxidation to NO_x led to adsorption on the silver surface, blocking the active sites for oxygen adsorption. The pathway for ammonia oxidation at low temperature was found to consist of a two-step consecutive reaction. Ammonia was first oxidized to NO. This

[1] To whom correspondence should be addressed. Fax: +31 40 245 5054. E-mail: l.gang@chem.tue.nl.

0021-9517/02 $35.00

reaction step was very fast on silver. At moderate temperatures (below 300°C) NO could then be removed either as N_2O or as N_2 through a surface SCR reaction, the second step of the reaction mechanism. At even higher temperatures. NO could directly desorb as one of the products. Apparently the ability of silver-based catalysts to perform the SCR reaction was closely related to its ability to oxidize ammonia.

As ammonia oxidation to nitrogen consists of two reaction steps and as it is difficult to find a catalyst that accelerates both of these, a composite catalyst system made of two or more catalyst components, each of which catalyzes only a part of the reaction, appeared to be a good alternative for improving the performance of the overall reaction. Hence a bifunctional catalytic system was sought.

The bifunctional catalyst required must first contain a component active for ammonia oxidation at low temperatures. The coproduction of N_2O can be avoided, or at least further reduced, by the second component, which performs the SCR of the intermediate NO species. As stated above, Ag is capable of performing the first step. Copper oxide appeared to be an excellent choice for the second component, as it is known to be both active and selective in the selective catalytic reduction of NO by ammonia. Supported copper oxide catalysts are commonly reported in the literature for this purpose (25). In addition, as previously mentioned, CuO yields a high selectivity to nitrogen in the SCO reaction. Alumina-supported Cu–Ag catalysts were thus prepared and screened for their ability to catalyze both the SCO and the SCR reactions. These materials were also characterized by several spectroscopic techniques in order to determine their physicochemical compositions and these were compared with catalytic performance. The results are discussed in this article.

2. EXPERIMENTAL

Ag/Al_2O_3, Cu/Al_2O_3, and $AgCu/Al_2O_3$ samples with different Ag and Cu loadings were prepared by incipient wetness (co-)impregnation. The precursors for these catalysts were $AgNO_3$ and $Cu(NO_3)_2$ distributed over the γ-Al_2O_3 support (Akzo/Ketjen 000 1.5E; surface area, 205 m^2/g). The samples were calcined in air at 500°C for 24 h before testing.

Catalytic activity measurements were carried out in a quartz, fixed-bed reactor (4-mm internal diameter). The amount of catalyst used was about 0.2 g (250 to 425–μm particles). Ammonia, oxygen, and helium flow rates were controlled by mass flow meters. NH_3, NO, and NO_2 were analyzed by a ThIs Analytical model 17C chemiluminescence NH_3 analyzer. Other substances such as N_2O, N_2, and H_2O were analyzed by a quadruple mass spectrometer (Baltzers OmniStar). The nitrogen mass balance was calculated based on a combination of these two analysis techniques (balance of $90 \pm 10\%$ for all the measurements).

High-resolution transmission electron microscopy measurements were performed using a Philips CM30/T at the National Centre for HREM at the Delft University of Technology. Samples were mounted on a microgrid carbon polymer supported on a copper grid, followed by drying at ambient conditions. EDX analysis was performed using a LINK EDX system. This enabled us to obtain information about the relative Ag/Cu ratios in selected areas of the sample.

X-ray powder diffraction (XRD) patterns were recorded on a Rigaku Geigerflex X-ray powder diffractometer using Cu $K\alpha$ radiation. Prior to the experiment, the catalysts were ground and pressed into a sample holder containing vaseline. The applied scanning speed was 1° per min. Background subtraction was not applied.

X-ray photoelectron spectroscopy (XPS) experiments were performed on a VG Ionex system modified with a VG Mg/Al $K\alpha$ X-ray source and a VG Clam II analyzer. The powdered catalyst particles were pressed into indium foil. To correct for the energy shift caused by charging, all peaks were corrected by setting the C 1s peak of adsorbed hydrocarbons to a binding energy of 285.0 eV. The peaks were fitted using the XPSPEAK version 4.0 peak-fitting program. All peaks were fitted by using a linear background.

Low-energy ion-scattering (LEIS) experiments were performed in co-operation with Calipso b.v. at the Eindhoven University of Technology. The newly developed ERISS system was used as the ion-scattering apparatus. In this apparatus ion doses can be reduced to such low levels that the damage to the surface is negligible, thus enabling the performance of static LEIS (15–20). To prevent charging of insulating materials, a neutralizer was available to spray low-energy electrons onto the sample. Samples were prepared by pressing the ground sample with a load of 1600 kg into a tantalum cup (ϕ, 1 cm) and subsequent loading into the pretreatment chamber that was connected to the main UHV chamber. All the samples were pretreated at 300°C in 214 mbar of oxygen for 20 min. Most LEIS measurements were performed using 5-keV Ne^+ ions; these provided a good mass resolution for the heavy elements (Ag and Cu). A number of samples were also analyzed using 3-keV $^4He^+$ ions. This yielded a good sensitivity for the light elements (C, O, Al, Si). In most cases, the samples were mechanically scanned over an area 1×1 mm^2 in size. During the measurements, the pressure in the main chamber was determined by the noble gas used in the ion source and was typically around 1×10^{-8} mbar. The base pressure of the system was in the 10^{-10} region. Analysis of the outermost surface layer and at different depths was performed on both the catalysts and on the gamma-alumina carrier. Depth analysis was performed by sputtering the samples with Ne^+ ions or $^4He^+$ ions, thus removing up to 8 monolayers (ML) with Ne^+ and up to 0.8 ML with $^4He^+$.

3. RESULTS

3.1. Catalytic Ammonia Oxidation Tests

Figure 1 shows the dependence of both ammonia conversion level and selectivity to nitrogen on the catalyst composition at 250°C. It can be seen that the conversion of ammonia increases with an increase in copper weight ratio in the catalyst, but that nitrogen selectivity changes in the opposite direction. It has previously been shown that selectivity is a very weak function of the ammonia conversion level (23). The optimum Ag/Cu weight ratio seems to be in the range between 1 and 3. Both activity and selectivity to nitrogen are high in this range. Apparently, nitrogen selectivity can be greatly improved by addition of small amounts of copper to the silver catalyst system, with only a small loss in catalyst activity.

For comparison, a mechanical mixture of 10 wt% Ag/Al_2O_3 and 10 wt% Cu/Al_2O_3 catalyst with a weight ratio of 3/1 was also tested in the SCO reaction. The results are listed in Table 1. It can be seen that a mechanically mixed silver and copper catalyst behaves similarly to the silver catalyst itself. Neither activity nor selectivity to nitrogen was improved by mechanical mixing of two different catalysts.

Figure 2 shows the conversion of ammonia and the selectivity to various products on an alumina-supported 7.5 wt% Ag–2.5 wt% Cu catalyst as a function of temperature. Between 200 and 300°C the catalyst converted 100% of the ammonia with a selectivity to nitrogen of circa 95%. Above 300°C, more NO_x is produced. The catalyst was quite stable. There was no significant deactivation during a one-day test under these experimental conditions. However, the selectivity did change somewhat with time (see Fig. 3). It can be seen from Fig. 3 that the selectivity to nitrogen increased with reaction time during the first 40 min on stream, whereafter it remained unchanged. This is mainly caused by adsorbed NO_x, N_2O_x species produced during reaction which can lower the surface oxygen coverage, as discussed previously (14).

TABLE 1

SCO ($NH_3 + O_2$) Reaction on Different Catalysts

Catalyst	Temperature (°C)	NH_3 conversion (%)	N_2 selectivity (%)
10 wt% Cu/Al_2O_3	250	12	97
	300	90	96
	350	100	90
10 wt% Ag/Al_2O_3	200	11	88
	250	98	86
	300	100	83
Ag/Al_2O_3 + Cu/Al_2O_3	200	8	89
(Ag/Al_2O_3 : Cu/Al_2O_3 = 3:1)	250	96	87
	300	100	82

Note. Reaction conditions: $NH_3 = 1.14\%$; $O_2 = 8.21$ vol%; flow rate = 74.7 N ml/min; catalyst weight = 0.2 g.

Selective catalytic reduction (SCR) of NO by ammonia was also tested on various copper- and silver-based catalysts to demonstrate the relationship between the SCR reaction and the ammonia oxidation reaction. Table 2 shows a comparison of the data obtained for the SCR reaction on different catalysts. It can be seen that the activity for the SCR reaction on the alumina-supported Cu–Ag catalyst was much higher than that on the alumina-supported silver catalyst. The SCR reaction was also more selective to nitrogen on the alumina-supported Cu–Ag catalyst as compared with alumina-supported silver catalysts.

3.2. XRD and XPS

Figure 4 shows the XRD diffractograms of 5 wt% Cu/Al_2O_3, 5 wt% Ag/Al_2O_3, and 7.5 wt% Ag–2.5 wt% Cu/

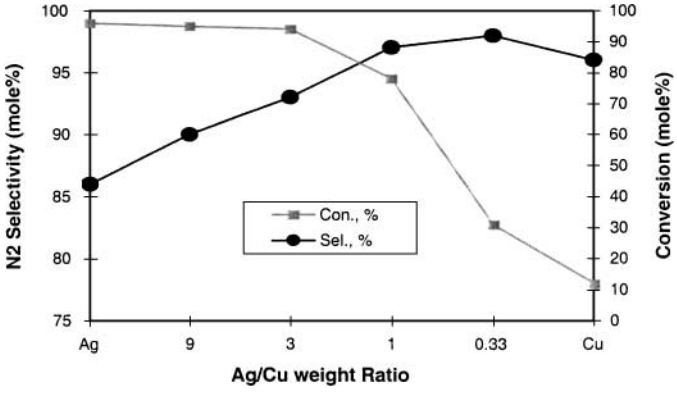

FIG. 1. The effect of Ag/Cu weight ratio on ammonia conversion and on selectivity to nitrogen for Ag–, Cu–, and AgCu/γ–Al_2O_3 catalysts. Reaction conditions: NH_3, 1.14 vol%; O_2, 8.21 vol%; flow rate = 74.7 N ml/min; catalyst weight = 0.2 g; $T = 250$°C.

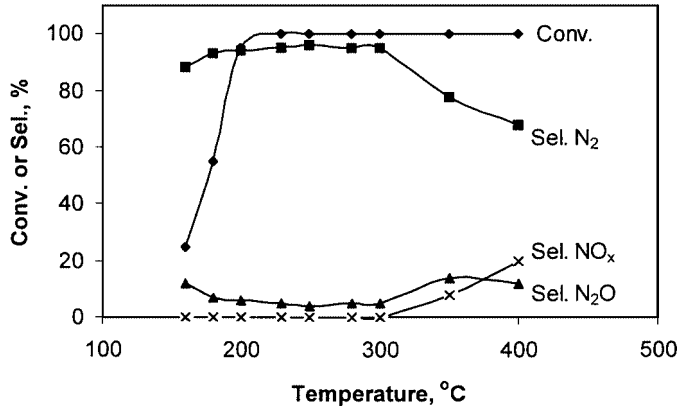

FIG. 2. Ammonia oxidation on 7.5 wt% Ag–2.5 wt% Cu/Al_2O_3 catalyst at various temperatures. Reaction conditions: $NH_3 = 1000$ ppm; $O_2 = 10$ vol%; total flow rate = 50 N ml/min; catalyst weight = 0.1 g.

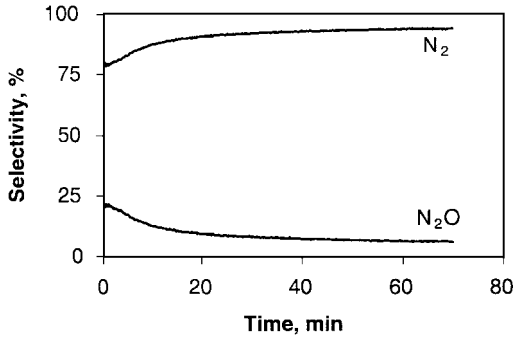

FIG. 3. Selectivity change with time on 7.5 wt% Ag–2.5 wt% Cu/Al_2O_3 catalyst. Reaction conditions: $NH_3 = 1000$ ppm; $O_2 = 10$ vol%; total flow rate = 50 N ml/min; catalyst weight = 0.1 g.

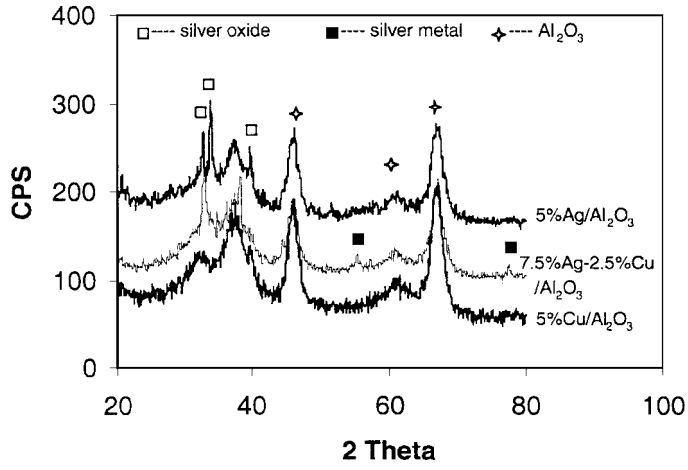

FIG. 4. XRD diffractograms of alumina-supported Cu–Ag catalysts calcined at 500°C.

Al_2O_3 catalysts. All the catalysts were calcined at 500°C in air for 24 h before measuring. No XRD diffraction lines attributable to crystallized copper metal or other copper compounds were observed on the copper-containing samples. However, diffraction lines attributable to AgO appeared in the XRD spectra of both silver-containing samples. Low-intensity diffraction lines due to metallic silver were also observed on the 7.5 wt% Ag–2.5 wt% Cu catalyst.

Four samples of Ag and Cu with different loadings of metal were characterized by XPS. The spectra in Fig. 5a show the Ag 3d region measured by XPS. Two peaks observed are due to removal of electrons from the $3d_{3/2}$ and $3d_{5/2}$ levels. The more intense peak due to removal of $3d_{5/2}$ core level electrons had a binding energy of 368.3 eV. Unfortunately, according to literature data (21), the binding energies of the 3d electrons in Ag^0, Ag^{+1}, or Ag^{+2} are all very similar. Hence it is impossible to ascertain the oxidation state of silver from this XPS peak alone. However, more information can be obtained by measuring the Auger bands to construct a Wagner plot (26). Figure 6 shows the Auger spectra obtained on three silver-containing catalysts in the region 370–330 eV. As shown, the peaks are very broad, but the kinetic energy of the Auger electrons is about 350 eV for all three samples. By comparison of these results with the literature (22) it can be concluded that silver is not in a metallic state, but in a state between Ag^{+1} and Ag^{+2}.

Figure 7 shows XPS spectra in the Cu 2p region (925–960 eV). The most intense peak occurs at about 932.5 eV. Comparing this result with literature data (21) it seems that Cu is in an oxidization state of +1 if copper is present as copper oxide since the 2p electrons in Cu^{+2} have a much higher binding energy (933.6 eV). Auger bands in the Cu region are shown in Fig. 8. The kinetic energies are circa 914 eV, much lower than that of CuO (918.1 eV) and Cu_2O (916.2 eV). The UV-spectra of our γ-alumina-supported copper catalysts (9) and extended X-ray absorption fine structure studies on other γ-alumina-supported copper catalysts (24) clearly showed that copper was in an oxidization state of +2. The shift of the binding energy may be

TABLE 2

SCR ($NO + NH_3$) Reaction on Different Silver-Based Catalysts

Catalyst	Temperature (°C)	NO conversion (%)	N_2 selectivity (%)
$CuAg/Al_2O_3$	150	27	98
(7.5% Ag–2.5% Cu)	200	61	95
	250	98	96
10 wt% Cu/Al_2O_3	150	53	98
	200	97	97
	250	99	98
10 wt% Ag/Al_2O_3	200	5	67
	250	14	74
	300	25	72

Note. Reaction conditions: NO = 500 ppm; $NH_3 = 1000$ ppm; $O_2 =$ 8 vol%; flow rate = 100 N ml/min; catalyst weight = 0.2 g.

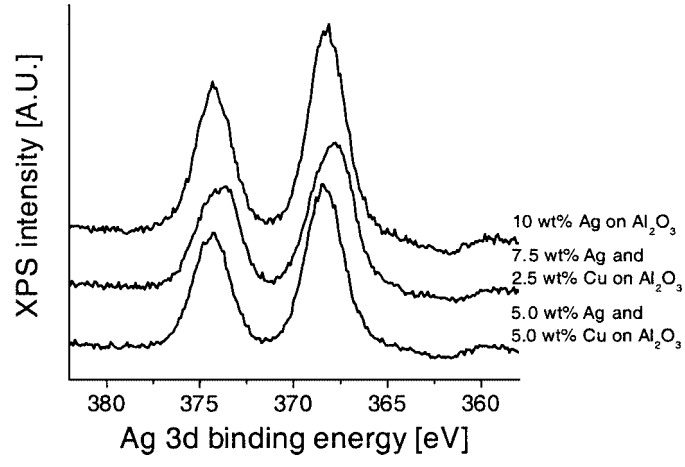

FIG. 5. Ag 3d XPS spectra of different Cu–Ag/Al_2O_3 catalysts.

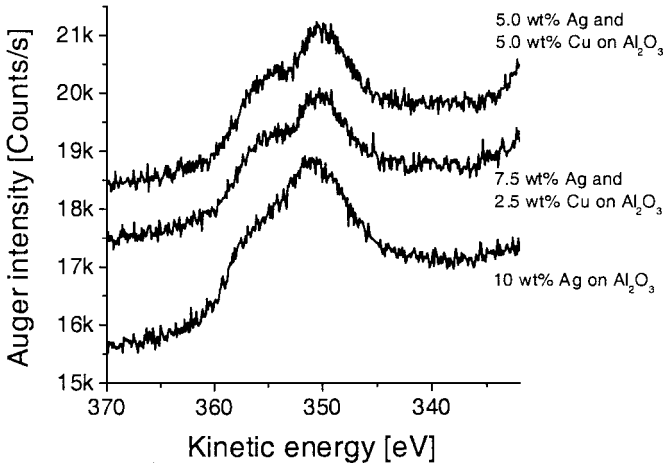

FIG. 6. Auger bands in Ag region for different Cu–Ag/Al_2O_3 catalysts.

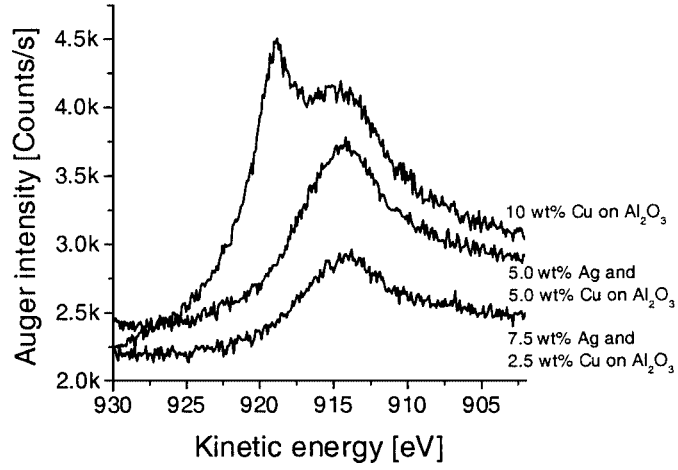

FIG. 8. Auger bands in Cu region for different Cu–Ag/Al_2O_3 catalysts.

caused by the interaction of copper with the support. New copper species other than copper oxide are formed due to this interaction. A second possibility is an interaction between Ag and Cu.

In order to be able to exclude any interaction between silver and copper two solid solutions were made of 5 wt% copper in silver and 5 wt% silver in copper. A special procedure was needed to fabricate these solid solutions, as at low temperatures these metals do not mix at all and will phase-separate into microcrystallites when cooling down from the melt. Such rough samples were prepared by melting the appropriate amounts together in an alumina crucible by induction in a high-frequency furnace, after which the samples were placed in two evacuated quartz capsules. These were heated for 96 h at a steady temperature of 800°C, at which temperature solid solutions of these compositions are possible, according to the phase diagram (27). Subsequent quenching prevented the formation of microcrystallites. The XPS spectra of the Ag 3d and Cu 2p did not show any difference from the pure metals after polishing. Any direct interaction between copper and silver, either through formation of an alloy or at boundaries, is thus very unlikely.

3.3. *LEIS Measurements*

The samples measured with LEIS are listed in Table 3. In addition to the Ag/Cu/γ-alumina catalysts, we analyzed a bare γ-alumina carrier material and Ag- and Cu-foil reference samples. Furthermore, in order to analyze the influence of surface roughness on the results we measured both a quartz sample and a silica carrier (Grace 332). Although these samples had the same elemental composition, quartz had a very smooth surface whereas the carrier material exhibits a much larger surface roughness (specific area of 235 m^2/g). Finally, an "ultra-pure" CuO powder sample was analyzed for quantification purposes. Figures 9 and 10

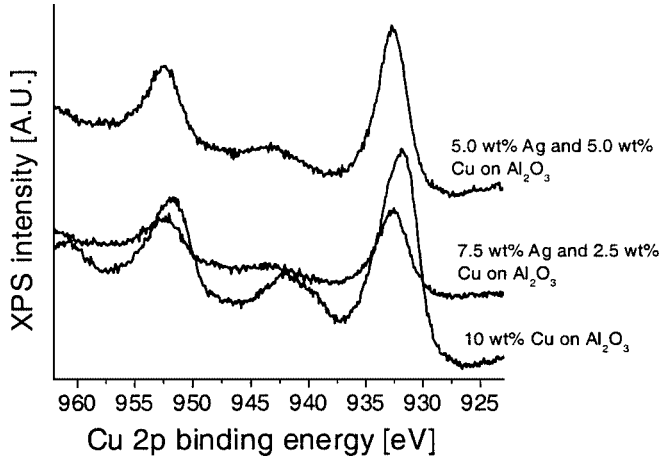

FIG. 7. Cu 2p XPS spectra of different Cu–Ag/Al_2O_3 catalysts.

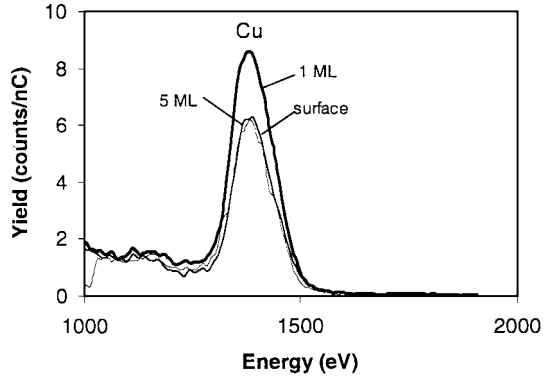

FIG. 9. 5 keV Ne^+ spectra of Cu/γ-alumina (5 wt% Cu) at different depths.

TABLE 3

Samples Analyzed by LEIS and Their Pretreatments

Sample	Ag (wt%)	Cu (wt%)	Pretreatment (in LEIS reaction chamber)	Ne^+ (5 keV)	$^4He^+$ (3 keV)
Cu/γ–alumina		5.0	214 mbar O_2, 300°C, 20 min	x	x
Ag/γ–alumina	10.0		213 mbar O_2, 300°C, 20 min	x	x
Ag/Cu/γ–alum.	10.0	2.5	212 mbar O_2, 300°C, 20 min	x	x
Ag/Cu/γ–alum.	2.5	7.5	201 mbar O_2, 300°C, 20 min	x	
Ag/Cu/γ–alum.	5.0	5.0	208 mbar O_2, 300°C, 20 min	x	
Ag/Cu/γ–alum.	9.0	1.0	210 mbar O_2, 300°C, 20 min	x	
γ–Alumina			216 mbar O_2, 300°C, 20 min		x
Reference Ag	100		Sputter-cleaned	x	x
Reference Cu		100	Sputter-cleaned	x	x
Quartz					x
Silica			Vacuum, 300°C, 74 min		x
CuO				x	

show the LEIS spectra of 5 wt% Cu/γ-alumina and 10 wt% Ag/γ-alumina samples as obtained with 5-keV Ne^+ ions. At the outermost atom layers of the samples significant Ag and Cu signals were detected.

The removal of the first (fraction of a) monolayer (ML) results in increased Ag and Cu signals. After a few MLs the intensities returned to a magnitude on the order of that of the outermost surface (Cu/γ-alumina) or slightly lower (Ag/γ-alumina). Most likely, the first ML removed consisted of contamination that had been deposited on the surface during the *in situ* calcination. The subsequent decrease in the signals suggests that prolonged sputtering resulted in smaller "accessible" silver and copper surfaces. Figure 11 shows one of the 5-keV Ne^+ spectra recorded for the bimetallic catalyst (10 wt% Ag–2.5 wt% Cu/Al_2O_3). In all cases, the removal of the first (fraction of a) ML resulted in increased intensities for both Ag and Cu. Again, we assume that we are dealing with surface contamination that, most likely, originated from the calcination of the samples.

Going deeper, down to 3–5 MLs, the respective Cu signals decreased in a similar fashion for all copper-containing samples. Concerning Ag, we observed a relatively large-intensity drop for the sample shown in Fig. 11. The 3-keV $^4He^+$ spectrum recorded for the 10 wt% Ag–2.5 wt% Cu/Al_2O_3 catalyst also shows the F peak originating from the bare carrier (Fig. 12).

The LEIS signals measured at 1-ML depth, i.e., after removal of surface contamination, contain information on the Ag and CuO dispersions. In order to obtain a (semi) quantitative picture of these dispersions, we have performed some calculations (see Table 4). Starting with the Cu signals, the results indicate that the CuO species are present as thin platelets with a thickness of roughly 1 ML. Between the samples, only minor differences are observed. Obviously, at increasing Cu loading, relatively more (or more extended) rather than thicker CuO platelets are formed. Based on surface-tension considerations, Ag is expected to form distinct particles on the γ-alumina support. Assuming (a) that these particles are spherical and (b) that only their upper halves contribute to the LEIS

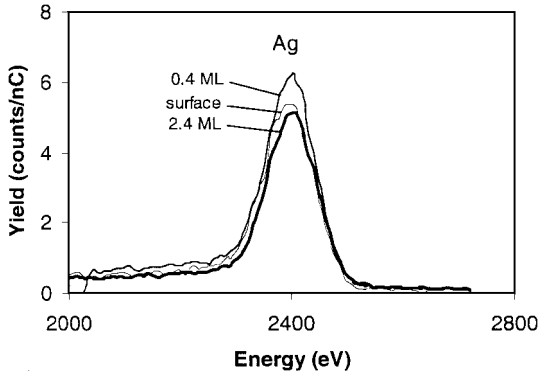

FIG. 10. 5-keV Ne^+ spectra of Ag/γ-alumina (10 wt% Ag) at different depths.

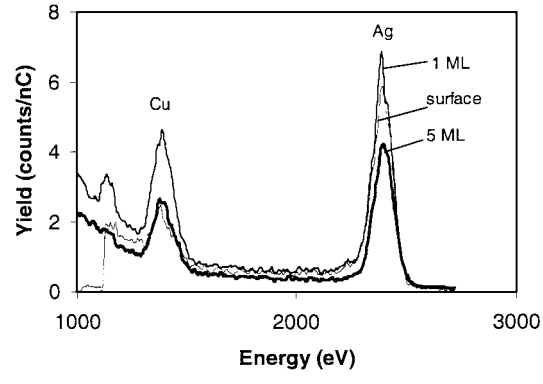

FIG. 11. 5-keV Ne^+ spectra of Cu/Ag/γ-alumina (2.5 wt% Cu, 10 wt% Ag) at different depths.

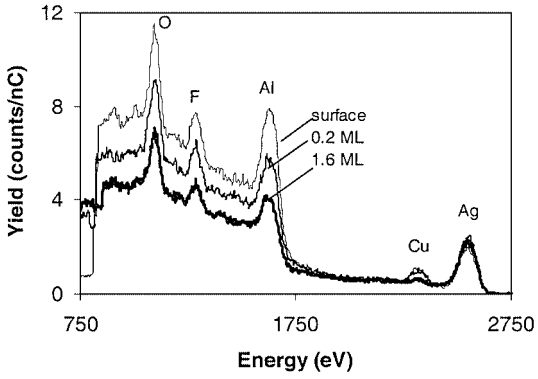

FIG. 12. 3-keV $^4He^+$ spectra of Cu/Ag/γ-alumina (2.5 wt% Cu, 10 wt% Ag).

signals, we calculate (from the "1-ML signals") that the average particle size of Ag ranges between 2.5 and 5.5 nm. Note that the numbers increase with an increase in Ag loading.

3.4. TEM and EDX Measurement

Single-component alumina-supported Cu and Ag catalysts with different loading were examined using transmission electron microscopy (TEM). No metal oxide particles were observed on the alumina surface of the 5 wt% Cu/Al_2O_3 and 10 wt% Cu/Al_2O_3 catalysts. Particles with diameters ranging between 5 and 10 nm were observed on the 15 wt% Cu/Al_2O_3 catalyst. The TEM images of the 5 wt% Ag/Al_2O_3 and 10 wt% Ag/Al_2O_3 catalyst seem to be similar. The silver particle size distribution was very broad. The smallest particles were about 1 nm in diameter; the largest particles found on the images were about 50 nm in diameter (see Fig. 13).

Two samples of mixed Cu–Ag/alumina catalysts were examined using TEM and EDX elemental analysis. Both samples contained a total metal loading of 10 wt%. One sample contained 7.5 wt% Ag and 2.5 wt% Cu. The other sample contained 2.5 wt% Ag and 7.5 wt% Cu.

7.5 wt% Ag–2.5 wt% Cu/Al_2O_3. This sample clearly consisted of two different macroscopic phases: one containing black particles and the other containing green particles. These two phases were mechanically separated (by hand) and were analyzed separately. Figure 14 shows a representative TEM image that was obtained for the fraction containing black particles. EDX analysis was performed at several different locations on the sample (see numbered arrows). Data points 1–4 were chosen to analyze areas containing dark particles. Data point 5 measured an area in which no dark particles were present. As the relative amounts of copper and silver are of importance these are shown in Table 5. Clearly the areas that include particles visible by TEM (points 1–4) contain very high amounts of silver relative to copper (circa 95:5). By contrast the area containing no visible particles (point 5, and others not shown here) contains relatively more copper than silver (circa 60:40).

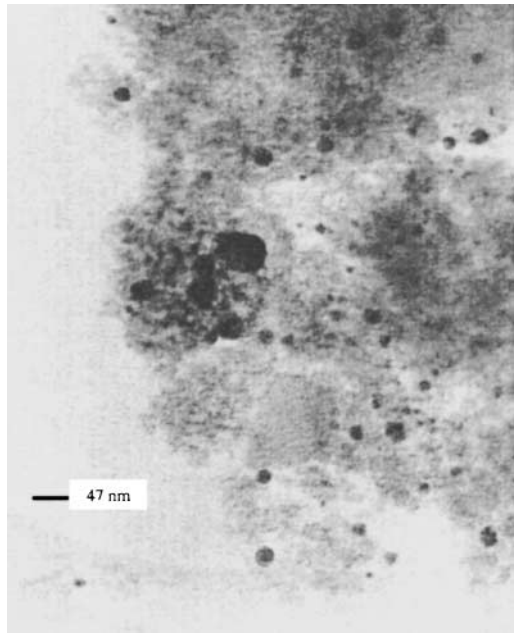

FIG. 13. TEM images of 10 wt% Ag/Al_2O_3 catalyst.

Figure 15 shows a TEM image that was obtained for the macroscopic green particles of this Ag-rich sample. The

TABLE 4

Calculation of CuO Platelets and Ag Particles Dispersion from LEIS Measurements

Catalysts			CuO platelets (depth: 1 ML)			Ag particles (depth: 1 ML)		
Cu (wt%)	Ag (wt%)	Ag/Cu (at/at)	Cu LEIS signal (cnts/nC)	Cu visible atoms (atoms/cm^2 × 10^3)	CuO platelets (thickness, MLs)	Ag LEIS signal (cnts/nC)	Ag visible atoms (atoms/cm^2 × 10^3)	Ag particles (av. size, nm)
1	9	5.3	231	5.4	0.8	728	4.1	4.1
2.5	10	2.4	352	8.2	1.2	645	3.6	5.2
5	5	0.6	895	20.8	1.0	510	2.8	3.2
7.5	2.5	0.2	1242	28.9	1.0	312	1.7	2.6

TABLE 5

Relative Amounts of Copper and Silver Measured by EDX on Different Areas of 7.5 wt% Ag–2.5 wt% Cu/Al_2O_3 (Black-Particle Fraction)

Data point	% atom Cu	% atom Ag
1	6.90	93.10
2	3.82	96.18
3	3.52	96.48
4	5.97	94.03
5 (area without dark particles)	59.70	40.30

Note. Data points refer to numbered arrows in Fig. 14.

TABLE 6

Relative Amounts of Copper and Silver Measured by EDX on Different Areas of 7.5 wt% Ag–2.5 wt% Cu/Al_2O_3 (Green-Particle Fraction)

Data point	% atom Cu	% atom Ag
1	1.02	98.98
2	1.10	98.90
3	2.10	97.90
4	1.10	98.90
5	1.68	98.32
6	0.86	99.14
7 (area without dark particles)	73.40	26.60

Note. Data points refer to numbered arrows in Fig. 15.

relative amounts of copper and silver (by EDX analysis) are listed in Table 6. Similar to the black-colored particle fraction, this phase also contained a wide distribution of particle size (up to 50 nm). These particles (data points 1–6) were slightly richer in silver relative to copper than were the black particles. Again although data point 7 shows no particles visible by TEM, both copper and silver were present, copper again being the more abundant.

7.5 wt% Cu–2.5 wt% Ag/Al_2O_3. Figure 16 shows a representative TEM image that was obtained for this Cu-rich sample. Again particles of a large distribution were observed. Table 7 shows the relative amounts of copper and silver measured at various locations. Again the darker particles visible by TEM (points 1–7) contain a larger abundance of silver. However in several locations the relative amount of copper to silver is higher than was observed in the previous samples. Data point 8 again shows that copper and a smaller amount of silver are present even in an area without visible dark particles.

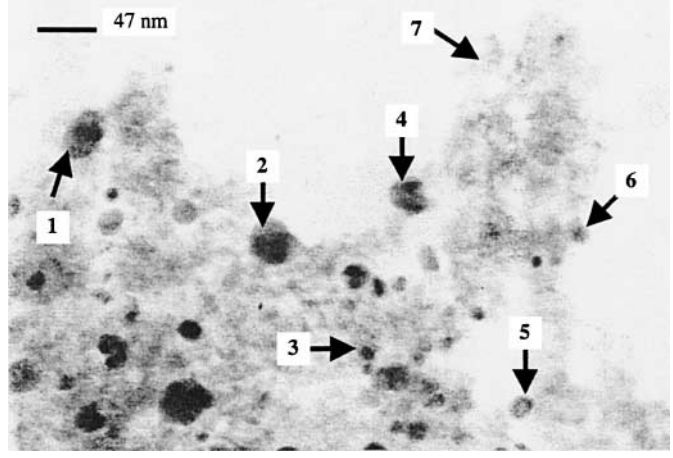

FIG. 15. TEM image of green particles of 7.5% Ag–2.5% Cu/Al_2O_3 catalyst (the arrows point to the area where the EDX measurement is performed).

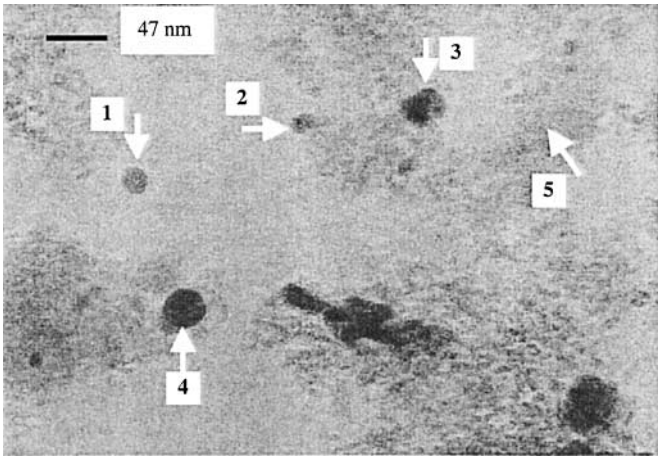

FIG. 14. TEM image of black particles of 7.5% Ag–2.5% Cu/Al_2O_3 catalyst (the arrow point to the area where the EDX measurement is performed).

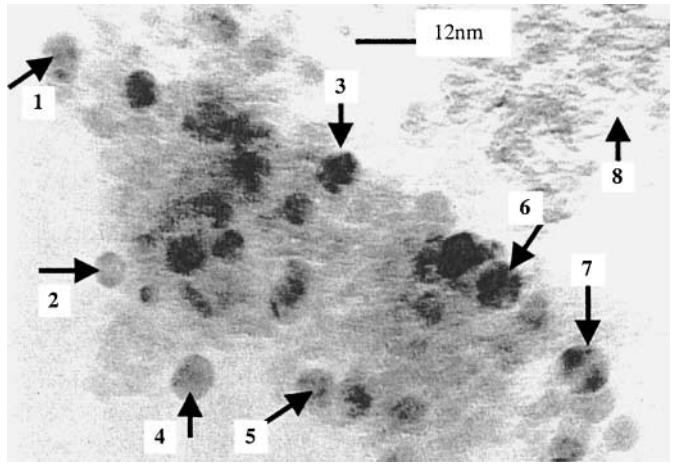

FIG. 16. TEM image of green particles of 2.5% Ag–7.5% Cu/Al_2O_3 catalyst (the arrows point to the area where the EDX measurement is performed).

TABLE 7

Relative Amounts of Copper and Silver Measured by EDX on Different Areas of 2.5 wt% Ag–7.5 wt% Cu/Al_2O_3

Data point	% atom Cu	% atom Ag
1	3.26	96.74
2	4.56	95.44
3	6.61	93.39
4	4.62	95.38
5	12.89	87.11
6	11.85	88.15
7	13.75	86.25
8 (area without dark particles)	83.28	16.72

Note. Data points refer to numbered arrows in Fig. 16.

4. DISCUSSION

Ammonia oxidation experiments have shown that silver alone supported on alumina has a very high ammonia oxidation activity but a low selectivity to nitrogen. Alumina-supported copper catalyst has a very high nitrogen selectivity but activity is low at low temperature. As discussed previously the aim of this study was to determine if alumina-supported binary Cu–Ag catalysts yield a higher selectivity to nitrogen without decrease in activity. The results show that this is indeed the case. Addition of Cu to Ag/Al_2O_3 catalysts, the incipient wetness coimpregnation, showed an increase in N_2 selectivity from 87 to circa 95% at 250°C while activity was not significantly reduced at Ag/Cu weight ratios greater than unity. An optimum ratio of between 1 and 3 was observed. The activity and selectivity to nitrogen for the SCR of NO by NH_3 were also increased following the addition of Cu. This is consistent with the previous observation that materials capable of catalyzing the SCO of NH_3 are also able to catalyze the SCR of NO by NH_3. This is due to the fact that the former reaction proceeds through an NO intermediate. Once formed the NO can be selectively reduced by NH_3 to nitrogen rather than being further oxidized to N_2O.

The fact is that a mechanical mixture of Cu/Al_2O_3 and Ag/Al_2O_3 catalysts, with an overall Ag/Cu ratio of 3 : 1, did not produce an increase in selectivity to nitrogen, as observed in the catalysts prepared by incipient wetness coimpregnation. The above result indicates that either close physical proximity or intimate chemical interaction between the silver and the copper components is necessary in order to increase selectivity. This can be understood by the fact that the intermediate NO cannot desorb from the catalyst surface at temperatures below 300°C, as shown previously (9). Thus at low temperatures, transport of NO between Ag and Cu must occur by surface diffusion.

In order to further understand the physicochemical nature of the $Cu–Ag/Al_2O_3$ catalysts the results of the various spectroscopic techniques must now be examined. XRD analysis of Cu/Al_2O_3 catalysts revealed that no peaks due to either metallic copper, copper oxide, or other copper compounds were present up to loadings as high as 10 wt%. TEM images of these catalysts also showed no visible particles. EDX analysis showed that copper was present on all areas of the alumina catalyst.

Based on the absence of distinct Cu particles in the TEM micrographs, it has been suggested that Cu might have reacted with (surface layers of) γ-alumina and formed $CuAl_2O_4$. However, the Cu atoms of this "normal spinel" component are known to occupy tetrahedral, i.e., subsurface, positions. Consequently, we would not expect $CuAl_2O_4$ to yield the large copper LEIS signals we actually have obtained. Former LEIS experiments performed on normal spinels yielded much smaller signals. Furthermore, small Cu (oxide) species may simply exhibit insufficient contrast (in TEM) when imaged on γ-alumina. The XRD results also show no diffraction line of $CuAl_2O_4$ phase for all the copper-containing samples. For these reasons, we judge the occurrence of spinels to be rather unlikely. Excluding the presence of spinels, Cu may be present either in metallic or in oxidic form. Following surface-tension considerations, metallic Cu species would form distinct particles whereas CuO species would wet the γ-alumina surface much better. The preparation of the catalysts (through wet impregnation of a mixture of Ag and Cu nitrates, followed by a reduction step) is expected to yield CuO species rather than metallic Cu particles. Furthermore, the catalysts were calcined prior to being analyzed with LEIS analysis. For these reasons, it is very likely that we are dealing with a CuO species. Although the expected form of copper oxide is Cu(II) oxide, XPS analysis of Cu/Al_2O_3 catalyst employing Wagnen plots revealed that copper is in an oxidation state of +1, thus suggesting the presence of Cu_2O.

Analysis of 5 and 10 wt% Ag/Al_2O_3 catalysts by TEM and EDX showed that Ag was always present as particles on the alumina surface. This is consistent with expectations based on surface tension between Ag and Al_2O_3. TEM revealed that a very wide particle distribution was always present (1–50 nm). XPS analysis of Ag/Al_2O_3 employing Wagnen plots showed that Ag was present in an oxidation state between +1 and +2. XRD analysis also showed the presence of AgO besides metallic silver. This is surprising, as Ag_2O is very unstable and AgO decomposes at 200°C, so that following calcination at 500°C metallic silver was expected.

TEM analysis of binary Cu–Ag catalysts revealed that a very large particle distribution was present (1–50 nm). EDX analysis revealed that the particles contained very large amounts of Ag relative to Cu. Areas in which no particles were present contained relatively more copper but still contained some silver. This suggests again that Cu was highly dispersed and that the particles were of Ag. Silver particles of very small diameters (<1 nm) must also be present. The observations by TEM are consistent with the results

of LEIS. A model generated suggested that copper oxide was highly dispersed, as a monolayer, and that the silver particles sit on top of this layer. The average Ag particle size for all silver-containing samples determined by LEIS was between 2.5 and 5.5 nm. The simple model predicts that the silver particle-size distribution is quite narrow and does not vary a lot among all the silver-containing catalysts. This distribution is much smaller than was observed by TEM. This probably arises from the fact that LEIS measures the silver content of the entire surface, thus including the small particles invisible to TEM.

XPS results show that the valence states of copper and silver are the same for single-component and bicomponent catalysts. The TEM images show very broad Ag particle-size distributions for all these catalysts. There is no indication for the formation of a new Cu–Ag phase. Indeed, as shown by the phase diagram (27), Ag and Cu have very low solubilities together at temperatures below 780°C. They tend to phase-separate at lower temperatures. There is no stable region in which a Cu–Ag alloy is formed.

As described previously, the ammonia oxidation on silver is a two-step reaction. Ammonia is first oxidized to NO and then the adsorbed NO is further reacted with NH_x to produce N_2. In a side reaction, NO can be oxidized to N_2O. The addition of copper to a silver catalyst enhances the selectivity of the SCR reaction. The promotional effect of copper can thus be well explained by a mechanism of bifunctional catalyst.

Since the NO produced in the first step of ammonia oxidation cannot desorb at low temperature, the copper and silver components should be in intimate contact with each other so that the NO produced on the silver surface can migrate to the copper surface easily. Otherwise, NO produced on the silver cannot reach the copper surface and the chances are greater that N_2O is produced rather than nitrogen. The EDX results showed that copper and silver existed together everywhere on the alumina surface. This proved that there was an intimate contact between copper and silver on alumina-supported Cu–Ag catalysts. Our experiments show that the performance of the catalyst, which is a physical mixture of 10 wt% Ag/Al_2O_3 and 10 wt% Cu/Al_2O_3, behaves similarly to the 10 wt% Ag/Al_2O_3 catalyst alone. This again confirms the importance of intimate contact between copper and silver.

In summary, copper was highly dispersed in all catalysts analyzed by LEIS and TEM. Most likely, the catalysts contain copper oxides platelets with a thickness of roughly 1 ML. At increasing copper loading, relatively more (or more extended) rather than thicker platelets are formed. However, silver has a broad particle-size distribution. The average size of the Ag species ranges between 2.5 and 5.5 nm, measured from LEIS. These numbers increase with an increase in silver loading. From TEM images silver is present as relatively large particles, with sizes ranging from 1 to 50 nm. The EDX results also show the existence of silver in the areas without dark particles. This indicates that a fraction of silver is dispersed in the form of platelets or very small particles that cannot be observed by TEM. This fraction of silver may be most interesting from a catalytic point of view. Unfortunately we still cannot unambiguously determine which fraction of silver plays the major role in ammonia oxidation at this stage.

Multifunctional catalysis is not a new concept, but a catalyst design deliberately based on the principle of multifunctionality will be necessary in order to develop high-performance catalysts which can cope with such difficult problems as those in ammonia oxidation. This study only gives one example of such a design. Actually there are more alternatives available. Besides silver, many noble metals, such as Pt and Ir, are very active for ammonia oxidation with low selectivity to nitrogen due to the low efficiency for SCR reaction. There are also many good SCR catalysts, such as vanadium oxide and iron oxide. Opportunities still exist for preparing high-performance bifunctional catalysts from these catalytic components.

5. CONCLUSIONS

Alumina-supported silver catalysts are very active for ammonia oxidation but N_2O is also coproduced on these catalysts. The addition of copper to these silver-based catalysts can greatly improved the catalytic selectivity to nitrogen with a negligible loss in activity for ammonia oxidation within the optimum Ag/Cu weight ratio range of between 1 and 3. XPS results show that the valence states of copper and silver are the same for single-component and bicomponent catalysts. LEIS and XPS measurements show no indication of formation of a new Cu–Ag phase. Such Cu–Ag alloys have been shown earlier to be thermodynamically unstable.

TEM images show the very broad particle-size distributions for all these catalysts. EDX results showed that copper and silver existed together everywhere on the alumina surface; thus intimate contact between copper and silver on alumina-supported Cu–Ag catalysts exists. All results seem to be consistent with a model that suggests that the catalyst structure consists of a highly dispersed (monolayer) of copper oxide on alumina upon which silver particles of a very wide particle-size distribution sit.

The promotional effect of copper can be explained by a bifunctional mechanism, in which the silver component mainly catalyzes ammonia oxidation to NO, the first step of this reaction, and the copper catalyzes the SCR of NO to nitrogen, thus reducing N_2O formation on silver.

ACKNOWLEDGMENTS

The authors kindly thank Mr. C. D. de Haan, National Centre for High Resolution Electron Microscopy, Delft University of Technology, The Netherlands, for assistance with the EDX measurements. The preparation

of the Cu(Ag) and Ag(Cu) solid solutions by Ir. M. J. H. van Dal is greatly appreciated. Financial support was provided by the Netherlands Technology Foundation (STW) and the Netherlands Organization for Scientific Research (NWO).

REFERENCES

1. van Loosdrecht, M. C. M., and Heijnen, S. J., *TIBTECH* **11**, 117 (1993).
2. Cole, J., *TIBTECH* **11** 368 (1993).
3. Amblard, M., Burch, R., and Southward, B. W. L., *Appl. Catal. B* **22**(3), L159 (1999).
4. Biermann, J. J. P., Ph.D. thesis. University of Twente, Twente, 1990.
5. de Boer, M., Huisman, H. M., Mos, R. J. M., Leliveld, R. G., Dillen, A. J., and Geus, J. W., *Catal. Today* **17**, 189 (1993).
6. Wollner, A., and Lange, F., *Appl. Catal. A* **94**, 181 (1993).
7. Li, Y., and Armor, J. N., *Appl. Catal. B* **13**, 131 (1997).
8. Sazonova, N. N., Simakov, A. V., and Veringa, H., *React. Kinet. Catal. Lett.* **57**(1), 71 (1996).
9. Gang, L., van Grondelle, J., Anderson, B. G., and van Santen, R. A., *J. Catal.* **186**, 100 (1999).
10. Ostermaier, J. J., Katzer, J. R., and Manoque, W. H., *J. Catal.* **41**, 277 (1976).
11. II'chenko, N. I., *Russ. Chem. Rev.* **45**, 1119 (1976).
12. van den Broek, A. C. M., Ph.D. thesis. Technical University of Eindhoven, Eindhoven, 1998.
13. Gang, L., van Grondelle, J., Anderson, B. G., and van Santen, R. A., Submitted for publication.
14. Gang, L., van Grondelle, J., Anderson, B. G., and van Santen, R. A., *J. Catal.* **199**, 107 (2001).
15. Hellings, G. J. A., Ottevanger, H., Boelens, S. W., Knibbeler, C. L. C. M., and Brongersma, H. H., *Surf. Sci.* **162**, 913 (1985).
16. Knibbeler, C. L. C. M., Hellings, G. J. A., Maaskamp, H. J., Ottevanger, H., and Brongersma, H. H., *Rev. Sci. Instrum.* **58**, 125 (1987).
17. Ackermans, P. A. J., van der Meulen, P. F. H. M., Ottevanger, H., van Straten, F. E., and Brongersma, H. H., *Nucl. Instrum. Methods Phys. Res. Sect. B* **35**, 541 (1988).
18. van Kessel, O., Brongersma, H. H., Hölscher, J. G. A., van Welzenis, R. G., Sengers, E. G. F., and Janssen, F. J. J. G., *Nucl. Instrum. Methods Phys. Res. Sect. B* **64**, 593 (1992).
19. Jacobs, J. P., Maltha, A., Reintjes, J. G. H., Drimal, J., Ponec, V., and Brongersma, H. H., *J. Catal.* **147**, 133 (1994).
20. Fullarton, J. C., Jacobs, J.-P., van Benthem, H. E., Kilner, J. A., Brongersma, H. H., Scanlon, P. J., and Steele, B. C. H., *Ionics* **1**, 51 (1995).
21. Moulder, J. F., Stickle, W. F., Sobol, P. E., and Bomben, K. D., *in* "Handbook of X-Ray Photoelectron Spectroscopy" (J. Chastain, Ed.), pp. 231–234. Perkin–Elmer, Eden Prairie, MI, 1992.
22. Briggs, D., and Seah, M. P. (Eds.), "Practical Surface Analysis by Auger and X-Ray Photoelectron Spectroscopy." Wiley, New York, 1983.
23. Gang, L., van Grondelle, J., Anderson, B. G., and van Santen, R. A., *Catal. Today* **61**, 179 (2000).
24. Friedman, R. M., Freeman, J. J., and Lytle, F. W., *J. Catal.* **55**, 10 (1978).
25. Armor, J. N., *Appl. Catal.* **1**, 221 (1992).
26. Wagner, C. D., Gale, L. H., and Raymond, R. H., *Anal. Chem.* **51**(4), 466 (1979).
27. Hansen, P. M., "Constitution of Binary Alloys." McGraw–Hill, New York, 1958.